Journal of Physics: Conference Series **97** (2008) 012231 doi:10.1088/1742-6596/97/1/012231

Design criteria for warm temperature dielectric superconducting dc cables: Impact of co-pole magnetic fields

P M Grant[1], W V Hassenzahl[2], B Gregory[3] and S W Eckroad[4]

[1]W2AGZ Technologies, San Jose, CA 95120 USA
[2]Advanced Energy Technologies, Oakland, CA USA
[3]Cable Consulting International, UK
[4]EPRI, Charlotte, NC 28262 USA

Corresponding author: P M Grant, w2agz@pacbell.net

Abstract. HTSC dc superconducting cables are under consideration for a variety of applications ranging from bi-directional interties between regional ac grids ("back-to-backs"), internal connection within, and out-feeds from, low voltage solar or wind farm generators, and up to multi-gigawatt transmission trunks linking remote nuclear clusters to urban load centers. In every instance, there are two principal design choices – coaxial, or "cold temperature dielectric; and mono-axial, also termed "warm temperature dielectric." In the former, both poles may be serviced by concentric conductors in the same physical package, separated by insulation held at the temperature necessary for superconducting operation, and in the latter, the poles are contained in two separate cables of more or less conventional design, each holding a cryostat enclosing the superconductor surrounded by a dielectric material at ambient temperature. Both have "pluses and minuses." CTD has the advantage of compactness, but requires a cryogenic dielectric, whereas WTD is simpler to manufacture and less costly overall as well. However, depending on the dimensional separation of the two poles and their containment infrastructure, WTD can experience considerable outward compressive physical forces and some reduction in critical state properties due to interpenetration of their respective magnetic fields. Recent progress in introducing homogeneous pinning in YBCO coated conductors could considerably ameliorate this latter issue, and thus the WTD design could engage a range of applications formerly out of reach of BSCCO tapes. We will examine these two issues in detail.

1. Introduction

Although the dream of using superconductors for the efficient transmission of electric power emerged almost immediately following its discovery in 1911, it was not until the 1960s that practical materials became available that made its realization feasible. One of the earliest superconducting cable design studies to be undertaken appeared in the 1967 paper by Garwin and Matisoo [1]. These authors addressed the overall physics and engineering issues confronted for a 100 GW $NbSn_3$ cable, 1000 km in length, carrying 500 kA at 200 kV for a total cost of 806 M USD (4990 M USD 2007). Their exercise was revisited by Grant [2] in the context of the present availability of high temperature superconducting tapes who concluded that Garwin-Matisoo scale HTSC cables were indeed viable, but at very high cost. Although their fabrication and installation may be physically plausible, it

remains to be seen whether deployment of such huge capacity corridors will take place over the coming decades.

We are thus motivated to consider nearer term, lower amperage designs for SCDC cables. It is likely that superconducting ac cables will be limited to 5 kA due to high hysteretic losses. On the other hand, in a dc cable it should be relatively straightforward to extend the current level to 10 kA dc, and perhaps 25 kA. Present superconducting ac cable configurations fall into essentially two categories depending on the temperature at which the high voltage dielectric is held. All coaxial designs incorporating a superconducting shield at either earth or opposing pole or phase potential require the dielectric to be at cryogenic temperature, hereafter referred to as CTD cables. All ac superconducting cable demonstration projects presently underway in the US are of this type [3, 4]. A simple SCDC CTD embodiment is described in [2] and an engineered model in [5] (by "engineered," we mean practical issues such as dimensions and materials packaging issues were addressed, not that a set of blueprints were produced.). The principal advantage of the CTD approach is the absence of external magnetic fields and forces due to screening by the shield. The principal disadvantages are size and cost, complexity of refrigeration, and uncertainties surrounding the high electric field breakdown properties of presently known dielectric materials at cryogenic temperatures.

2. Warm temperature dielectric superconducting power cables

On the other hand, once given the discovery of high temperature superconductors and their subsequent development into long length high performance tapes, along with operation at or near liquid nitrogen temperatures allowing more optimum management of heat in-leak losses, it became possible to consider configurations where the cryogenic shield could be eliminated. This permitted a rather simple design whereby a conventional high voltage transmission cable in which the central copper conduct is replaced by a "cryostat" comprising a superconductor core surrounded by a concentric vacuum package and superinsulation within a flexible stainless steel corrugated tube. This tube would be at earth or neutral potential, thus accommodating an outer sheath of conventional high voltage dielectric at ambient temperature, or "warm temperature," WTD or "room temperature," RTD. The first engineered WTD cable design was developed by EPRI [6], shown in figure 1 below.

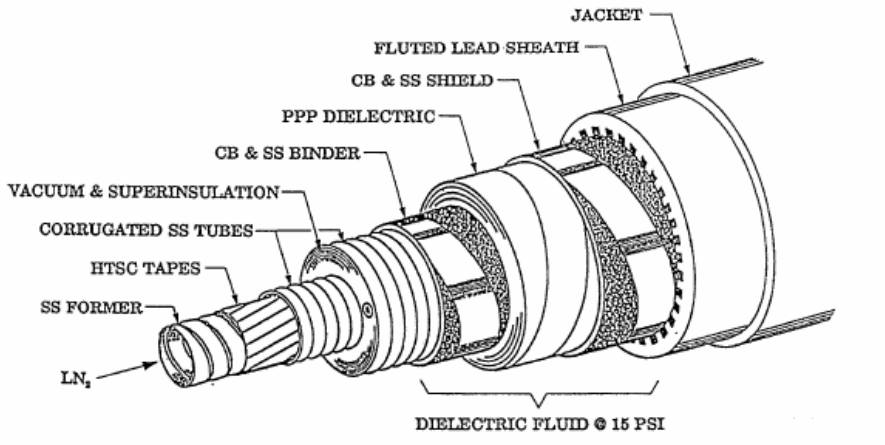

Figure 1. The 1994 EPRI WTD cable [6]. Note the cryogen, here liquid nitrogen, flows through the cross-section normally occupied by the copper conductor in a conventional cable.

This concept became the basis of several HTSC cable prototype demonstrations not only in the US, but in Europe and China as well. Details of these efforts can be found in reference [4]. Of special interest to the subject of this paper are the projects undertaken by EPRI and Pirelli [7], the Detroit-Edison Frisbie Substation demonstration [8], and by Innopower at Puji Substation in Kunming [9]. The advantages of the WTD approach are simplicity of manufacture, reduction of footprint and cost (half the superconducting tapes per given capacity are required compared to CTD), and, especially for ac, and opportunity for retrofitting presently installed urban transmission cables. Principal disadvantages are societal perceptions of the danger, real or imaginary, of unshielded power line magnetic fields, and more realistically, the deleterious effect of such fields emanating from co-pole or co-phases on the performance of intrinsically anisotropic HTSC conductors, and the considerable magnetic forces impressed on these neighbors as a result of their respective increased current capacities. Focus on these last two subjects will occupy the rest of this paper.

We begin by identifying three key geometric parameters essential to their examination, as shown in figure 2, along with their numerical values summarized in table 1 for the three WTD projects identified above.

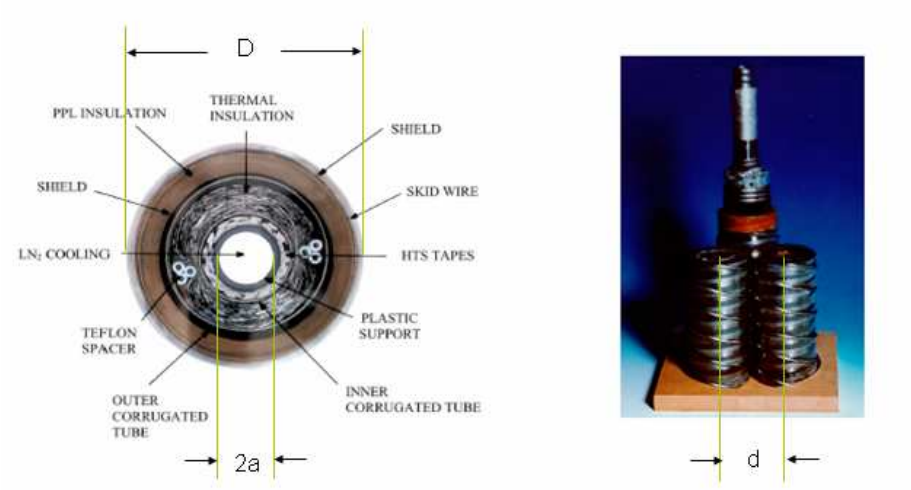

Figure 2. Key parameters critical to estimating magnetic field and force issues endemic to WTC cables in both ac and dc circuits. The image on the left is an actual cross-section of the original EPRI/Pirelli 50-m prototype tested in 1998 [7] and more or less reflects the absolute dimensions, D, the overall cable diameter, and a, the superconductor former radius, of other WTC designs (see table 1). On the left is the original model of the Pirelli "cable-in-conduit retrofit," indicating the distance d between co-poles or co-phases of neighboring WTC cables in the network.

Table 1. Specifications and geometric parameters of past WTD cable projects.

Cable Project	V (kV)	I (A)	D (mm)	a (mm)	d (mm)
EPRI/Pirelli [7]	115	2000	88.1	18.6	95
DTE Frisbie [8]	25	2400	88.1	18.6	254
Puji Substation [9]	35	2000	112.0	17.5	1000

Of special significance to inter-WTD cable fields and forces is *d*, the conductor – conductor, center-to-center distance. The governing equations for these quantities derive from Ampere's and Lorentz' Laws respectively:

$$B = \frac{\mu_0}{2\pi}\frac{I}{r}, \tag{1}$$

$$\frac{dF}{dl} = \frac{\mu_0}{2\pi}\frac{I^2}{r}, \tag{2}$$

where *B* is the magnetic field at a distance *r* (in this case, *r* = *d*) from a long cylindrical conductor carrying a current *I*, and *dF/dl* is the repulsive force per unit length (hereafter all references to "force" will be assumed normalized to unit length) between two such conductors carrying opposing and equal in magnitude currents. In SI units, $\mu_0/2\pi = 2 \times 10^{-7}$ T·m·A^{-1}. It is known that co-phase induced hysteretic losses in a three-phase ac WTD circuit can be substantial when the cables are close together. A team at Los Alamos National Laboratory found in measurements made at 60 Hz where two of the phases were simulated by copper bus bars at a 95 mm distance from a bare HTSC multi-tape conductor in the relative geometry of the model in figure 2, that its hysteretic losses were 2-3 times higher at 1000 A(rms) than when energized alone [7]. However, when a direct current of 1000 A was substituted for ac in the two copper bus bars, the overall performance as measured by the decrease in critical current, was degraded only by about 5%. As far as we know, the reason for the large effect of co-phase ac currents on hysteretic losses remains ill understood.

Inasmuch as we address the possible use of WTD cables for transport of direct current several times greater than the rms values typical of the demonstrations listed in table 1, it is important to note (see equations (1) and (2)) that the magnetic field goes linearly with *I* and the force quadratically for a given cable separation distance, *d*. Depending on the magnitude of the latter, the inter-cable force can be tens of "g's" (gravities, 1 g = 9.81 N), and thus could impose a serious constraint on the design of the cryostat portion of WTD cables.

3. Magnetic fields and forces between two parallel conductors

Figure 3 depicts the Biot-Savart (integral form of Ampere's Law) solution for the total magnetic field of two parallel cylindrical conductors of radius *a* separated a distance *d* carrying equal and opposing currents *I*. Hereafter, unless otherwise noted, we take units of magnetic field as $\mu_0/2\pi(I/a)$ T, and *x, y* as proportional to *a*. The inter-conductor distance is *d* = 5*a*, representative of the dimensions of EPRI/Pirelli WTD prototype shown in figure 2. The value *d/a* = 5 is likely to be the low-limit practical value for separation of two adjacent WTD cables.

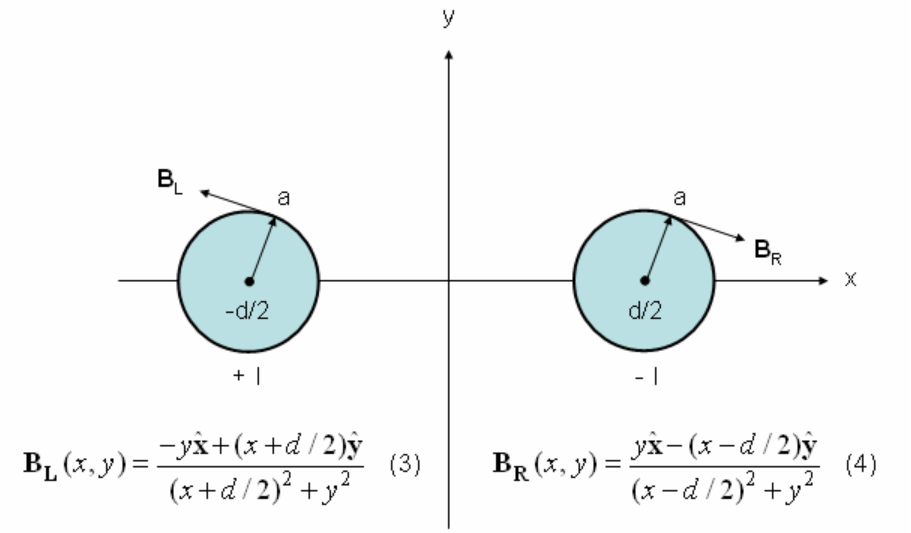

$$\mathbf{B}_{\mathbf{L}}(x,y)=\frac{-y\hat{\mathbf{x}}+(x+d/2)\hat{\mathbf{y}}}{(x+d/2)^2+y^2} \quad (3) \qquad \mathbf{B}_{\mathbf{R}}(x,y)=\frac{y\hat{\mathbf{x}}-(x-d/2)\hat{\mathbf{y}}}{(x-d/2)^2+y^2} \quad (4)$$

$$\mathbf{B}(x,y)=\mathbf{B}_{\mathbf{L}}(x,y)+\mathbf{B}_{\mathbf{R}}(x,y) \quad (5)$$

Figure 3. Explicit Biot-Savart equations for the total vector magnetic field of two parallel cylindrical conductors of radius *a* separated a distance *d* carrying equal and opposing currents *I*. Units of magnetic field are $\mu_0/2\pi(I/a)$ T, and *x*, *y* are proportional to *a*. Figure is drawn to scale taking $d = 5a$. The right-hand-rule applies.

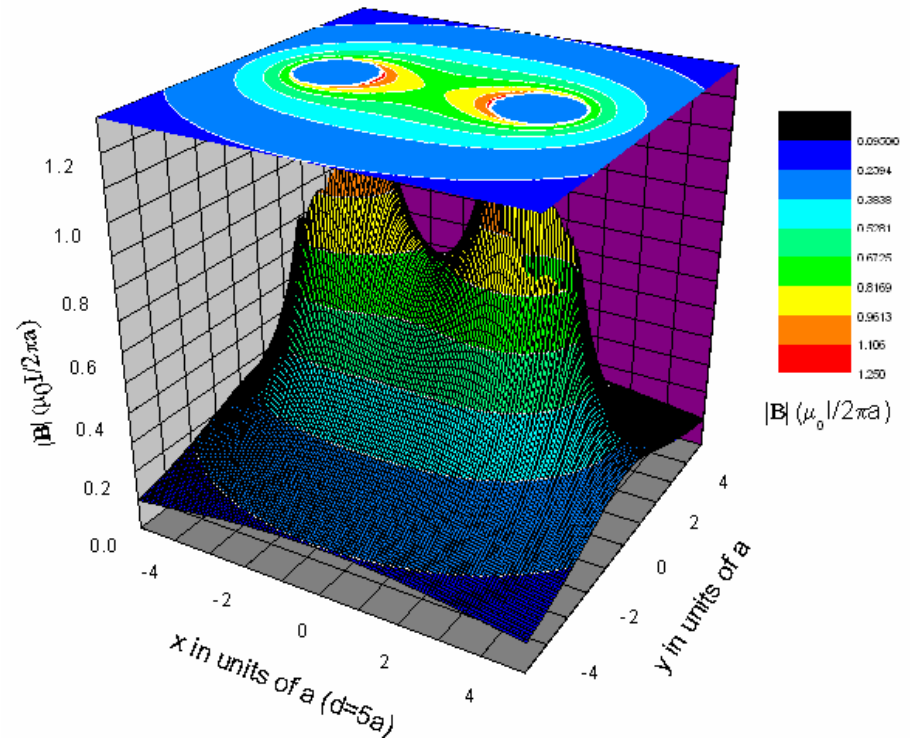

Figure 4. Surface and contour plots for the magnetic field and force field amplitudes resulting from equations (5) and (2).

In figure 4, we present the results for the magnitude of the total magnetic field given by equation (5), and also contour details of $B(x,y)$ near the surface of both conductors. We note that approaching the surface of each conductor, there is a rather salubrious cancellation of much of the incoming co-pole field by the respective self-fields arising from the opposing current flows, and that the angle of intersection of the field with the conductor surfaces, as shown by the contours of constant field, is likewise reduced. We also note that from Lorentz' Law, equation (2), the magnetic field amplitudes shown in figure 4 are also proportional to the force field amplitude per unit conductor length (but not its directional components!) in units of $\mu_0/2\pi(I^2/a)$ N.

Next we compute from the data of figure 4, the angle of incidence of **B** and its magnitude, and the magnitude of the normal component of the Lorentz force around the circumference of each conductor. The methodology is given in figure 5, using the "right hand" conductor of figure 3, and the results given and discussed in section 4 to follow.

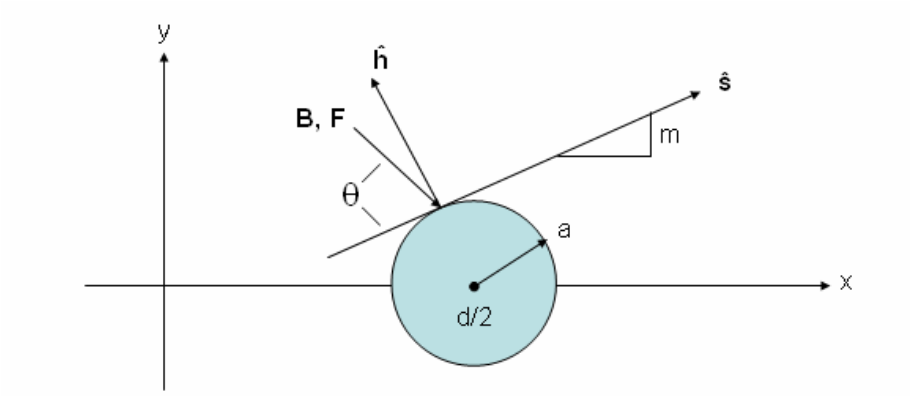

$$\left.\begin{aligned} y &= \pm\sqrt{a^2+(x-d/2)^2} \\ m &= \pm\frac{dy}{dx} = \frac{-(x-d/2)}{y} \\ \hat{\mathbf{s}} &= \frac{\hat{\mathbf{x}}+m\hat{\mathbf{y}}}{\sqrt{1+m^2}},\quad \hat{\mathbf{h}} = \frac{-m\hat{\mathbf{x}}+\hat{\mathbf{y}}}{\sqrt{1+m^2}} \end{aligned}\right\} \quad (6)$$

$$\theta = \cos^{-1}\frac{\mathbf{B}\bullet\hat{\mathbf{s}}}{|\mathbf{B}|} \quad (7)$$

$$F_h = \mathbf{F}\bullet\hat{\mathbf{h}} \quad (8)$$

Figure 5. Matrix algebra methodology for calculation of the magnetic field angle of incidence, θ, and the normal Lorentz force, F_h, on the surface of the conductors, here expressed explicitly for the right-hand conductor.

4. Results and discussion

Figure 6 shows the results obtained from the data of figure 4 and the analysis of figure 5. Figure 6 does not explicitly give the surface dependence of the normal Lorentz force, F_h. A detailed analysis of equations (2), (6) and (8) for $d/a > 3$ will show the scaling factor on the right hand y axis for $|\mathbf{B}|$ in dimensionless units, $\mu_0/2\pi(I/a)$ T, is numerically equivalent within 2% for F_h relative to newton units, $\mu_0/2\pi(I^2/a)$ N. We will use this fact in calculations displayed and discussed later in table 2. We see

that for d/a = 5, the crossing of angle of incidence and maximum magnetic field magnitude is around 9 degrees from the tangent to the conductor surface and may be considered a "worst case" scenario as regards reducing its critical current performance due to the co-pole field. However, the actual situation is rather more subtle as the field intensity varies over the conductor surface as well as angle. Thus, one should take into account variation of the electric field, E, versus current density, J, and associated power law parameters with magnetic field. At this time, we know of no such measurements on YBCO tape, or empirical estimates, and will leave such as an exercise for the future.

However, we can make some rough estimates using existing data for critical current versus angle at constant field, as given in figure 7 [10]. We have found such data can be fit to a general expression of the form:

$$I_{C-W}(\theta) = G_c(\theta) I_{base} + (I_c - I_{base}) G_c(\theta) + (I_{ab} - I_{base}) G_{ab}(\theta) \ ,$$
where $G_n(\theta)$ has the form (9)
$$G_n(\theta) = \exp[-(\theta - \theta_n)^2 / 2\sigma_n^2] \ .$$

The parameters appropriate to figure 7 are given in the insets. We find equation (9) to be quite general, and fits well even in rare cases where I_{ab} or $I_c < I_{base}$.

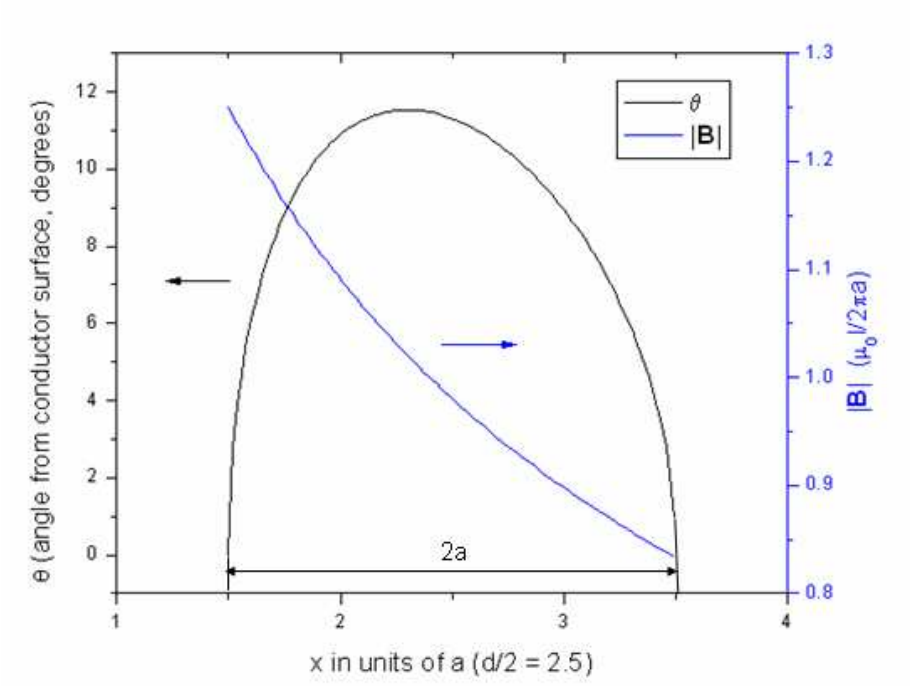

Figure 6. Plot of θ and magnetic field magnitude, |**B**|, over the surface of one of the pairs of a two-pole configuration of WTD neighboring cables. See figure 5 and text for details of the calculation and description of units.

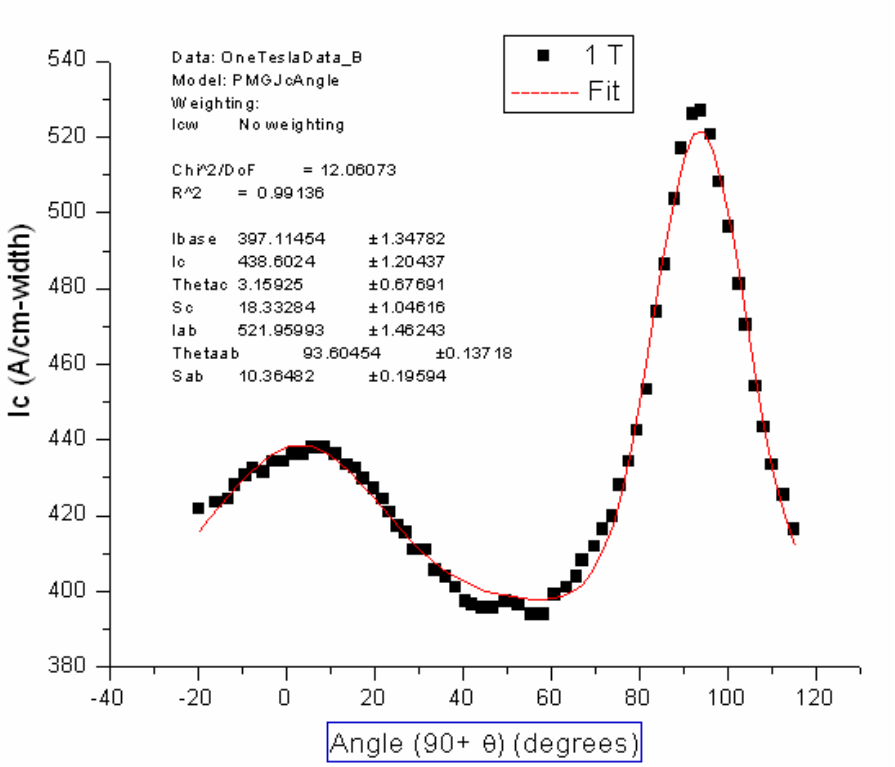

Figure 7. $I_{C\text{-}W}(\theta)$ in a field of 1 T at 65 K for YBCO deposited via PLD on RABiTS-ed substrates [10] fit to equation (9). See inset for details.

In fact, we would suggest the parameters involved in equation (9) and indeed its actual "gauss-base" functional behavior may reflect some of the physics of the distribution and "coherency" of the pinning defects and provides an interesting subject of investigation. Similar ideas have also been discussed by Civale, *et al.*, [11] in terms of simple FWHM measurements.

We see 9 degrees off the I_{ab} peak yields only around a 10% degradation in critical current (in fact, at the "valley of death" 40 degrees away it is a tolerable 25%); however, the data we use were taken in a 1 T field, and such high fields generally reduce the anisotropy with angle of $I_{C\text{-}W}(\theta)$ and, as can be seen from a glance at table 2, are also much greater than likely to be experienced in any given pairing of WTD cables, even when transporting 25 kA. Having said that, not much is known about $I_{C\text{-}W}(\theta)$ in practical coated conductors in fields of 0.05 – 0.1 T since it is seldom measured. Some of the measurements made at 0.5 T reported in reference [11] suggest the degradation with small angles off θ_{ab} might be considerable.

Table 2. Magnetic fields and forces between WTD cables as a function of separation.

Cable Project	I (A)	d/a	B(a) (T)	B(d) (T)	B(d)/B(a)	dF/dl (g/m)
EPRI/Pirelli	2000	5.11	0.022	0.004	0.20	0.86
DTE Frisbie	2400	13.66	0.026	0.002	0.07	0.77
Puji Substation	2000	57.14	0.023	0.0004	0.02	0.08
EPRI/Pirelli	10000	5.11	0.108	0.021	0.20	21.5
DTE Frisbie	10000	13.66	0.108	0.008	0.07	8.03
Puji Substation	10000	57.14	0.114	0.002	0.02	2.1
EPRI/Pirelli	25000	5.11	0.269	0.053	0.20	134.1
DTE Frisbie	25000	13.66	0.269	0.020	0.07	78.7
Puji Substation	25000	57.14	0.286	0.005	0.02	12.7

On the other hand, the inter-cable conductor repulsive forces for currents of order 25 kA present a significant challenge, even for *d*'s on the scale of the DTE and Puji demonstrations. The reason can be seen quite clearly from figure 1 and the cable cross-section on the left hand side of figure 2. The force on each conductor pushes it outward against the soft thermal superinsulation between it and the wall of the cryostat, likely crushing it and giving rise to a "thermal short" and rendering it useless. On the other hand, structural plastics and metals can readily withstand 10^6 or more. The early Garwin-Matisoo concept envisioned Nb_3Sn conductors with a = 12.6 mm carrying 500 kA at d = 40 mm apart (d/a = 3.17) would produce conductor surface fields and center-to-center values of 8 and 2.5 T, respectively, and a repulsive force exceeding one million g. Their design was not WTD, but two conductors immersed in liquid helium within a stainless steel or aluminum tube. Each conductor was coated with a solid polymer dielectric and the authors maintained both the dielectric and metal cylinder would withstand such enormous forces.

5. Conclusions

In this paper we have considered design issues raised for WTD dc HTSC cables by the inter-conductor fields on mutual critical current degradation and repulsive forces. We conclude the former is manageable, especially given the ongoing improvement in isotropic pinning in REBCO coated conductors, but the latter will require new and innovative cryostat architectures.

References

[1] Garwin R L and Matisoo J 1967 J *Proc. IEEE* **55** 538
[2] Grant P M 2007 *IEEE Trans. Appl. Supercon.* **17**(2) 1641
[3] http://www.oe.energy.gov/DocumentsandMedia/superconBROCHURE2.pdf.
[4] http://www.w2agz.com/asc06.htm.
[5] Chowdhuri P, Pallem C, Demko J A and Gouge M J 2005 *IEEE Trans. Appl. Supercon.* **15** 3917
[6] Engelhardt J Design concepts for a superconducting cable *EPRI Report TR-103631(September 1994)*
[7] Nassi M Superconducting cable construction and testing *EPRI and DOE Final Report 1000160 (November 2000)*
[8] Kelly N and Eckroad SW (2003) Field demonstration of a 24-kV warm dielectric superconducting cable at Detroit Edison *EPRI and DOE Report 1002040*
[9] Xin Y 2003 *Reported at EUCAS 2003*
[10] Kang S, *et al.* 2006 *Science* **311** 1911
[11] Civale L, *et al.* 2004 *Appl. Phys. Lett.* **84** 2121
[12] Guetiérrez J, *et al.* 2007 *Nature Materials* **6** 367